

# Fine-Grained Human Pose Editing Assessment via Layer-Selective MLLMs

Ningyu Sun<sup>1</sup>, Zhaolin Cai<sup>1</sup>, Zitong Xu<sup>1</sup>, Peihang Chen<sup>1</sup>,  
Huiyu Duan<sup>1</sup>, Yichao Yan<sup>1</sup>, Xiongkuo Min<sup>1\*</sup> Xiaokang Yang<sup>1</sup>

<sup>1</sup>Institute of Image Communication and Network Engineering, Shanghai Jiao Tong University  
{jiaotong870810, xuzitong, ph4.66, huiyuduan, yanyichao, minxiongkuo, xkyang}@sjtu.edu.cn

**Abstract**—Text-guided human pose editing has gained significant traction in AIGC applications. However, it remains plagued by structural anomalies and generative artifacts. Existing evaluation metrics often isolate authenticity detection from quality assessment, failing to provide fine-grained insights into pose-specific inconsistencies. To address these limitations, we introduce **HPE-Bench**, a specialized benchmark comprising 1,700 standardized samples from 17 state-of-the-art editing models, offering both authenticity labels and multi-dimensional quality scores. Furthermore, we propose a unified framework based on layer-selective multimodal large language models (MLLMs). By employing contrastive LoRA tuning and a novel layer sensitivity analysis (LSA) mechanism, we identify the optimal feature layer for pose evaluation. Our framework achieves superior performance in both authenticity detection and multi-dimensional quality regression, effectively bridging the gap between forensic detection and quality assessment.

**Index Terms**—Pose editing, image quality assessment, multimodal large language model

## I. INTRODUCTION

The rapid evolution of text-guided image editing has transformed content creation, empowering users to manipulate visual semantics through natural language prompts [1]–[3]. Specifically, human pose editing has emerged as a pivotal research area, allowing for the precise alteration of a subject’s action or posture [4]. Distinct from general style transfer, pose editing necessitates strict adherence to structural integrity and spatial geometry. While state-of-the-art diffusion models have achieved milestones, they remain prone to generative artifacts, including limb distortions and unnatural texture blending, which undermine the utility and authenticity of the results.

Pose editing introduces both security concerns, as models may generate unrealistic or harmful manipulations [5], [6], and quality concerns, since users expect visually natural and instruction-consistent results [7]. Forensic methods can identify manipulated content but do not capture perceptual quality [8], whereas IQA metrics assess visual fidelity but fail to detect subtle fabricated details [9], [10]. In practice, authenticity analysis and quality assessment can reinforce each other, since a deeper understanding of forensic features helps expose unrealistic pose constructions that degrade quality, while quality measurements offer fine-grained feedback that facilitates the detection of subtle, imperceptible manipulations. Whereas these two aspects are inherently interconnected and

mutually beneficial, an evaluation framework that integrates forensic detection with quality assessment is meaningful.

To this end, we introduce **HPE-Bench** (illustrated in Fig. 1), a fine-grained benchmark for human pose editing. HPE-Bench comprises 1,700 standardized samples generated by 17 SOTA editing models, spanning both description-based and instruction-based paradigms. Unlike previous datasets that offer only single-dimensional ratings, HPE-Bench provides a rich set of annotations, including authenticity labels for forensic analysis and fine-grained scores in perceptual quality, editing alignment, and attribute preservation. This benchmark serves as a foundational platform for developing evaluation metrics tailored to the complexities of pose synthesis.

Building upon HPE-Bench, we propose a unified framework for authenticity detection and quality assessment, leveraging layer-selective multimodal large language models (MLLMs). Our approach is grounded in the insight that forensic traces are coupled with perceptual quality, the same generative artifacts that expose inauthenticity also degrade visual fidelity. To exploit this correlation, we employ contrastive LoRA tuning to align MLLM representations, maximizing the feature distance between authentic and edited poses. Furthermore, to address the variability of feature distributions, we introduce a layer sensitivity analysis (LSA) mechanism. This module automatically identifies the most informative feature layers by computing statistical metrics, including KL divergence, local discriminant ratio, and feature entropy. Through targeted adaptation, our framework achieves robust performance in both forensic detection and quality assessment tasks.

Our main contributions are as follows:

- We construct HPE-Bench, the first fine-grained human pose editing benchmark featuring 1,700 standardized samples from 17 generative models with authenticity labels and multi-dimensional quality annotations.
- We propose a unified framework based on layer-selective multimodal large language models, which integrates contrastive LoRA tuning and a novel layer sensitivity analysis mechanism to extract robust discriminative features.
- We achieve superior performance in authenticity detection and multi-dimensional quality assessment, effectively bridging the gap between forensic detection and perceptual evaluation in human pose editing.

\* Corresponding Author

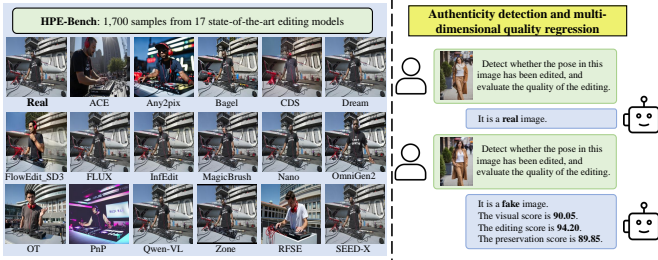


Fig. 1. Overview of our constructed HPE-Bench and the proposed evaluation task. HPE-Bench contains 1,700 standardized samples generated by 17 diverse state-of-the-art editing models. Our unified framework performs concurrent authenticity detection and multi-dimensional quality regression, providing scores for visual quality, editing alignment, and attribute preservation.

## II. CONSTRUCTION OF HPE-BENCH

To support evaluation of fine-grained human pose editing, we construct HPE-Bench, a benchmark emphasizes structural pose transformations, where the human body's geometric configuration is edited while non-target attributes are expected to remain consistent. Each sample is a triplet  $(I_{src}, I_{edit}, T)$ , where  $I_{src}$  denotes the authentic source image,  $I_{edit}$  is the pose-edited image generated by editing model, and  $T$  represents the pose transformation prompt. This formulation enables both real-fake discriminative learning and instruction-aware quality evaluation within a unified benchmarking framework.

### A. Image Collection and Prompt Engineering

1) *Source Data Curation*: We collect high-resolution real-world images containing human subjects with clear and well-defined body structures to ensure suitability for pose-driven editing. To ensure precise pose estimation, samples exhibiting severe occlusion, truncation, or ambiguous configurations were excluded. A minimum resolution threshold of  $1024 \times 1024$  pixels was enforced to preserve structural fidelity, serving the purpose of high-quality generation and forensic evaluation.

2) *Prompt Formulation*: For each source image, we generate pose-editing prompts based on images using a MLLM. Each prompt defines the target transformation while enforcing semantic consistency for invariant attributes. To avoid physically implausible motions and ill-defined editing objectives, all prompts are refined through rule-based screening and manual verification. The resulting instruction set encompasses a broad spectrum of modification scenarios, ranging from action transitions to human-object interaction adjustments.

### B. Standardized Generation Protocol

1) *Generative Models*: We select 17 representative text-guided image editing models spanning both instruction-based and description-based paradigms to cover a broad range of pose-editing behaviors and artifact patterns. Instruction-driven methods include IP2P [2], MagicBrush [3], Any2Pix [11], ZONE [12], HQEdit [13], and ACE++ [1], while description-based approaches include Text2LIVE [14], EDICT [15], DDPM [16], MasaCtrl [17], CDS [18], PnP [19], InfEdit [20], ReNoise [21], RFSE [22], FlowEdit (SD3) [23], FlowEdit

(FLUX) [23]. These models differ substantially in their generative mechanisms, including diffusion-based generation, rectified flow modeling, and inversion-based control, resulting in diverse pose deformation patterns and artifact distributions.

2) *Data Synthesis and Analysis*: For each of selected editing models, we apply curated source images and corresponding prompts to generate pose-edited samples, resulting in exactly 100 edited images per model and 1,700 samples in total. To characterize the statistical properties of the generated data, we analyze low-level feature distributions across real and edited images. Results indicate that pose-edited images generally exhibit reduced spatial information but increased colorfulness and contrast, which is consistent with patterns observed in generic manipulation datasets. These deviations further confirm that pose editing introduces detectable structural and textual artifacts, motivating the use of robust representation learning for both detection and quality assessment.

### C. Metadata Acquisition and Annotation

We conduct human evaluation under a controlled setup to obtain reliable subjective annotations for pose editing quality. Annotations are performed using python interface on  $3840 \times 2160$  resolution monitor. A total of 20 trained annotators participate in the evaluation process, with samples presented in randomized order and annotation sessions divided into short rounds to mitigate visual fatigue and scoring bias.

Each edited image is annotated following a three-stage protocol consisting of labeling, cross-verification, and expert arbitration to ensure annotation reliability. Annotators provide assessments across three dimensions. Perceptual quality ( $S_q$ ) measures visual fidelity and penalizes visible generative artifacts. Editing alignment ( $S_e$ ) evaluates the semantic consistency between the edited pose and the textual instruction. Attribute preservation ( $S_p$ ) assesses whether non-target regions including background context and identity-related attributes remain unaffected. Beyond these fine-grained metrics (on a 1-5 scale), each sample is also assigned a binary authenticity label to support supervised forensic detection.

## III. PROPOSED METHOD

### A. Overview

We propose a unified framework designed to simultaneously assess the authenticity and quality of pose-edited images. Given a triplet  $\{I_{src}, I_{edit}, T\}$ , where  $I_{src}$  is the source image,  $I_{edit}$  is the edited image, and  $T$  is the textual instruction, our objective is to predict a binary authenticity label  $y_{auth}$  and a multi-dimensional quality vector  $y_{qual} = [s_q, s_e, s_p]^\top$ . The architecture is built upon a multimodal large language model (MLLM). To overcome the insensitivity of pre-trained MLLM to high-frequency manipulation traces, we introduce contrastive Low-Rank Adaptation (LoRA). Furthermore, to balance forensic discriminability with semantic richness, we propose a layer sensitivity analysis (LSA) mechanism that selects the optimal feature layer. Finally, the selected features feed into specific decoders for detection and regression.

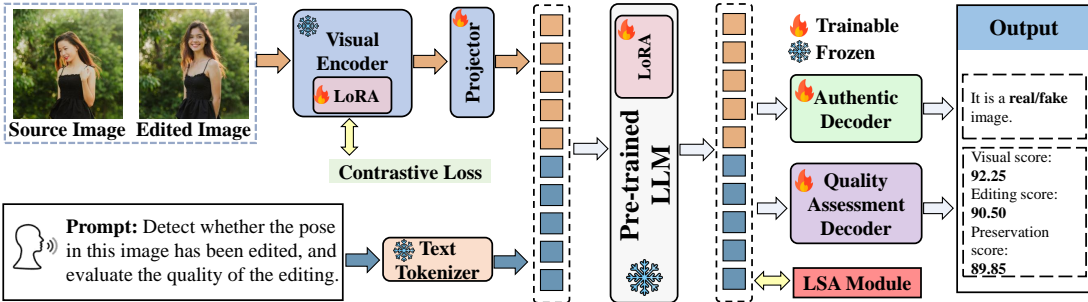


Fig. 2. Overview of our proposed framework. The model employs a contrastive LoRA tuning strategy on visual encoder and MLLM to enhance sensitivity to pose-editing artifacts. A layer sensitivity analysis (LSA) module computes statistical metrics to select the optimal intermediate feature layer from the MLLM. Finally, the authentic decoder and quality assessment decoder are utilized for simultaneous authenticity detection and multi-dimensional quality scoring.

### B. Contrastive Visual Tuning

Standard MLLM prioritize semantic alignment over high-frequency artifact detection. To address this, we apply LoRA tuning, injecting trainable rank decomposition matrices to adapt features for forensic sensitivity without catastrophic forgetting. To explicitly shape the latent space, we minimize a supervised contrastive loss  $\mathcal{L}_{con}$  using triplets of real anchor  $f_{src}$ , positive real  $f_{pos}$ , and negative edited  $f_{edit}$ :

$$\mathcal{L}_{con} = -\log \frac{\exp(\text{sim}(f_{src}, f_{pos})/\tau)}{\sum_{f \in \{f_{pos}, f_{edit}\}} \exp(\text{sim}(f_{src}, f)/\tau)} \quad (1)$$

This objective forces the MLLM to cluster real samples while pushing manipulated ones apart, amplifying feature disparity caused by pose artifacts.

### C. Layer Sensitivity Analysis (LSA)

MLLM representations are hierarchical, shallow layers capture low-level patterns, while deeper layers encode abstract semantics [57], [58]. Effective pose assessment requires a trade-off, sufficient low-level detail for artifact detection and high-level semantics for quality evaluation. We introduce LSA to profile each layer  $l$  and select the optimal depth  $L_{opt}$ . The selection criterion  $S(l)$  aggregates three normalized metrics:

- **Distributional Shift ( $D_{KL}$ ):** We measure the Kullback-Leibler divergence between the feature distributions of real ( $P_{real}$ ) and edited ( $P_{edit}$ ) samples. High divergence indicates strong sensitivity to manipulation:

$$D_{KL}^{(l)} = \sum_x P_{real}^{(l)}(x) \log \frac{P_{real}^{(l)}(x)}{P_{edit}^{(l)}(x)} \quad (2)$$

- **Class Separability (LDR):** To quantify discriminative power, we compute the Local Discriminant Ratio, defined as the ratio of between-class variance to within-class variance across feature dimensions  $D$ :

$$LDR^{(l)} = \frac{1}{D} \sum_{d=1}^D \frac{(\mu_{real,d} - \mu_{edit,d})^2}{\sigma_{real,d}^2 + \sigma_{edit,d}^2 + \epsilon} \quad (3)$$

- **Information Richness ( $E$ ):** We calculate the Shannon entropy of feature activations ensuring the layer retains sufficient information for complex quality regression:

$$E^{(l)} = - \sum_i p(h_i) \log p(h_i) \quad (4)$$

The optimal layer is selected via  $L_{opt} = \text{argmax}_l (\hat{D}_{KL}^{(l)} + \hat{LDR}^{(l)} + \hat{E}^{(l)})$ , where  $\hat{\cdot}$  denotes min-max normalization. We utilize the hidden state  $H^{(opt)}$  from this layer as the input for subsequent tasks.

### D. Task-Specific Inference

Leveraging the optimal representation  $H^{(opt)}$ , we employ two decoder to handle the distinct nature of authenticity detection and quality assessment tasks.

1) *Authenticity Detection*.: A multilayer perceptron maps  $H^{(opt)}$  to a probability score  $\hat{y}_{auth}$ . This decoder is supervised by the binary cross-entropy loss  $\mathcal{L}_{det}$ , learning to distinguish between pristine and edited imagery.

2) *Quality Regression*.: To assess perceptual and semantic quality, a multi-head regression network projects  $H^{(opt)}$  into three scalar scores including perceptual quality ( $\hat{s}_q$ ), editing alignment ( $\hat{s}_e$ ), and attribute preservation ( $\hat{s}_p$ ). We optimize this decoder using the Mean Squared Error (MSE) loss:

$$\mathcal{L}_{qual} = \frac{1}{N} \sum_{i=1}^N \|\hat{y}_{qual}^{(i)} - y_{qual}^{(i)}\|_2^2 \quad (5)$$

This design enables the model to correlate specific manipulation artifacts with degradation in human perceptual ratings.

## IV. EXPERIMENTS

### A. Experimental Setup

We utilize the InternVL3.5 backbone [55]. HPE-Bench is split 4:1:1 (train/val/test). We use AdamW with cosine annealing. LoRA and decoders are trained with learning rates of  $1 \times 10^{-4}$  and  $5 \times 10^{-5}$ , respectively. Evaluation metrics include Accuracy/F1 for detection, and Spearman ( $\rho_s$ ), Kendall ( $\rho_k$ ), and Pearson ( $\rho_p$ ) correlations for quality assessment.

### B. Authenticity Detection Performance

1) *Comparison with Specialized Detectors*: As presented in Table III-B, our framework outperforms all deepfake detection methods (♡) and AI-generated image detectors (♣). Compared with the strong baseline AIDE, our method establishes new state-of-the-art performances. This advantage is observed consistently across instruction-based and description-based editing models, indicating that the learned representation is robust to different pose-editing generation mechanisms.

TABLE I

COMPARISON RESULTS ON DIFFERENT MANIPULATION METHODS. ♠ STANDARD CNN/TRANSFORMER BASELINES, ♡ DEEPCODE DETECTION METHODS, ♣ AI-GENERATED IMAGE DETECTION METHODS, ♢ MULTIMODAL LARGE LANGUAGE MODELS. THE FINE-TUNED RESULTS ARE MARKED WITH \*. THE BEST RESULTS ARE HIGHLIGHTED IN **RED**, AND THE SECOND-BEST RESULTS ARE HIGHLIGHTED IN **BLUE**.

Editing Model Model/Metric	Text2LIVE		EDICT		IP2P		DDPM		MasaCtrl		CDS		MagicBrush		PnP		Any2Pix	
	Acc↑	F1↑	Acc↑	F1↑	Acc↑	F1↑	Acc↑	F1↑	Acc↑	F1↑								
Random Choice	50.00	50.00	50.00	50.00	50.00	50.00	50.00	50.00	50.00	50.00	50.00	50.00	50.00	50.00	50.00	50.00	50.00	50.00
♡MVSSNet* [5]	57.50	66.67	62.50	59.63	65.00	78.79	67.50	82.35	60.00	70.97	56.25	64.41	61.25	73.02	65.00	78.79	60.00	70.97
♡PSCCNet* [6]	50.00	82.35	40.00	66.67	46.25	76.92	38.75	64.41	45.00	75.00	46.25	76.92	45.00	75.00	38.75	64.41	43.75	73.02
♡HifiNet* [24]	66.25	82.35	60.00	68.55	68.75	83.71	57.50	68.55	61.25	75.00	66.67	55.00	64.41	55.00	64.41	68.75	85.71	
♣FakeShield* [8]	72.50	84.00	77.50	90.41	73.75	85.71	70.50	90.41	72.50	84.06	71.25	82.35	71.25	82.35	73.75	85.71	75.00	87.32
♣CNNSpot* [25]	58.75	73.02	63.75	80.60	61.25	76.92	58.75	73.02	65.00	82.35	63.75	80.60	62.50	78.79	58.75	73.02	60.00	75.00
♣Lagrad* [26]	65.00	78.79	70.00	<b>85.71</b>	62.50	75.00	61.25	73.02	66.25	80.60	66.25	80.60	63.75	76.92	73.75	90.41	66.25	80.60
♣Univ* [27]	73.75	87.32	71.25	84.06	76.25	90.41	68.75	80.60	72.50	85.71	75.00	88.89	75.00	88.89	66.25	76.92	73.75	87.32
♣AIDE* [28]	<b>83.75</b>	<b>91.89</b>	<b>76.25</b>	82.35	<b>86.25</b>	<b>94.74</b>	<b>80.65</b>	<b>87.32</b>	<b>82.50</b>	<b>90.41</b>	<b>88.75</b>	<b>97.44</b>	<b>83.75</b>	<b>91.89</b>	<b>86.25</b>	<b>94.74</b>		
☆LLaVA-1.6 (7B) [29]	53.75	66.67	56.25	70.97	51.25	62.07	51.25	62.07	62.50	80.60	57.50	73.02	51.25	66.67	62.50	80.60		
☆LLaVA-NeXT (8B) [30]	70.97	57.50	80.60	63.75	78.79	62.50	62.07	52.50	90.41	71.25	84.06	66.25	76.92	61.25	84.06	66.25	78.79	62.50
☆mPLUG-Owl3 (7B) [31]	47.50	66.67	52.50	75.00	58.75	84.00	47.50	66.67	62.50	88.89	42.50	57.14	57.50	82.35	47.50	66.67	60.00	85.71
☆LLama3.2-Vision (11B) [32]	67.50	84.06	57.50	68.85	63.75	78.79	62.50	76.92	65.00	80.60	61.25	75.00	65.00	80.60	57.50	68.85	61.25	75.00
☆MiniCPM-V2.6 (8B) [33]	55.00	66.67	63.75	80.60	62.50	78.79	52.50	62.07	66.25	84.06	50.00	57.14	58.75	73.02	58.75	73.02	55.00	66.67
☆Ovis2.5 (9B) [34]	42.50	54.55	43.75	57.14	47.50	64.41	48.75	66.67	47.50	64.41	53.75	75.00	53.75	75.00	40.00	49.06	53.75	75.00
☆DeepSeekVL2 (small) [35]	58.75	75.00	73.02	83.75	61.25	78.79	61.25	78.79	53.75	66.67	62.50	80.60	61.25	78.79	53.75	66.67	62.50	75.00
☆InternVL3.5 (8B) [36]	46.25	54.55	56.25	73.02	53.75	68.85	51.25	64.41	56.25	73.02	51.25	64.41	57.50	75.00	51.25	64.41	57.50	75.00
☆Qwen3-VL (8B) [37]	67.50	80.60	56.25	62.07	65.00	76.92	61.25	70.97	62.50	73.02	70.00	84.06	68.75	82.35	60.00	68.85	62.50	73.02
Ours	<b>94.74</b>	<b>90.00</b>	<b>93.33</b>	<b>87.50</b>	<b>96.10</b>	<b>92.50</b>	<b>98.73</b>	<b>97.50</b>	<b>94.74</b>	<b>90.00</b>	<b>97.44</b>	<b>95.00</b>	<b>96.10</b>	<b>92.50</b>				
Editing Model Model/Metric	InferEdit		ZONE		ReNoise		HQEdit		RFSE		FlowEdit(SD3)		FlowEdit(FLUX)		ACE++		Overall	
	Acc↑	F1↑	Acc↑	F1↑	Acc↑	F1↑	Acc↑	F1↑	Acc↑	F1↑								
Random Choice	50.00	50.00	50.00	50.00	50.00	50.00	50.00	50.00	50.00	50.00	50.00	50.00	50.00	50.00	50.00	50.00	50.00	50.00
♡MVSSNet* [5]	57.50	66.67	53.75	59.63	63.75	76.92	65.00	78.79	67.50	82.35	68.75	84.06	65.00	78.79	67.50	82.35	62.57	74.74
♡PSCCNet* [6]	51.25	84.06	41.25	68.85	40.00	66.67	57.50	91.89	55.00	88.99	50.00	82.35	52.50	85.71	46.25	76.92	46.32	76.47
♡HifiNet* [24]	60.00	73.02	65.00	80.60	62.50	76.92	63.75	78.79	71.25	88.89	62.50	76.92	60.00	84.06	62.50	76.92	62.87	77.02
♣FakeShield* [8]	71.25	83.75	66.25	75.00	72.50	84.06	67.50	76.92	78.75	91.89	82.50	96.10	75.00	87.32	76.25	88.89	73.82	85.58
♣CNNSpot* [25]	60.00	75.00	61.25	76.92	61.25	76.92	67.50	85.71	61.25	76.92	70.00	88.89	67.50	85.71	66.25	84.06	62.79	79.03
♣Lagrad* [26]	68.75	84.06	57.50	66.67	66.25	80.60	67.50	82.35	68.75	84.06	65.00	78.79	72.50	<b>88.89</b>	68.75	84.06	66.47	80.65
♣Univ* [27]	63.75	73.02	68.75	80.60	<b>77.50</b>	<b>91.89</b>	72.50	85.71	76.25	90.41	71.25	84.06	73.75	87.32	76.25	90.41	72.50	85.50
♣AIDE* [28]	<b>86.25</b>	<b>94.74</b>	<b>78.75</b>	<b>85.71</b>	76.25	82.35	<b>83.75</b>	<b>91.89</b>	<b>86.25</b>	<b>94.74</b>	<b>85.00</b>	<b>95.33</b>	<b>77.50</b>	84.06	<b>83.75</b>	<b>91.89</b>	<b>82.79</b>	<b>90.58</b>
☆LLaVA-1.6 (7B) [29]	57.50	73.02	58.75	75.00	57.50	73.02	57.50	73.02	67.50	87.32	66.25	85.71	65.00	84.06	58.60	74.21		
☆LLaVA-NeXT (8B) [30]	85.71	67.50	68.85	56.25	87.32	68.75	90.41	71.25	88.89	70.00	85.71	67.50	88.89	70.00	93.33	73.75	82.10	65.22
☆mPLUG-Owl3 (7B) [31]	55.00	78.79	51.25	73.02	53.75	73.75	62.50	88.89	61.25	87.32	56.25	80.60	62.50	88.89	58.75	84.06	55.15	78.33
☆LLama3.2-Vision (11B) [32]	63.75	78.79	63.75	78.79	66.25	82.35	63.75	78.79	70.00	87.32	73.75	91.89	67.50	84.06	75.00	93.33	65.00	80.23
☆MiniCPM-V2.6 (8B) [33]	66.25	84.06	57.50	70.97	57.50	70.97	61.25	76.92	65.00	82.35	68.75	87.32	66.25	84.06	66.25	84.06	60.66	75.46
☆Ovis2.5 (9B) [34]	53.75	75.00	41.25	51.85	50.00	68.85	58.75	82.35	55.00	76.92	56.25	78.79	56.25	82.35	50.66	69.18		
☆DeepSeekVL2 (small) [35]	62.50	80.60	67.50	87.32	55.00	68.85	61.25	78.79	67.50	87.32	71.25	91.89	63.75	82.35	61.25	78.79	61.40	78.67
☆InternVL3.5 (8B) [36]	53.75	68.85	61.25	80.60	62.50	82.35	55.00	70.97	53.75	68.85	56.00	70.97	57.50	75.00	55.29	71.12		
☆Qwen3-VL (8B) [37]	66.25	78.79	65.00	76.92	70.00	84.06	61.25	70.97	73.75	88.89	65.00	76.92	67.50	80.60	72.50	87.32	65.59	77.43
Ours	<b>97.44</b>	<b>95.00</b>	<b>90.41</b>	<b>82.50</b>	<b>97.44</b>	<b>95.00</b>	<b>95.00</b>	<b>97.44</b>	<b>95.00</b>	<b>93.33</b>	<b>87.50</b>	<b>87.50</b>	<b>97.44</b>	<b>95.00</b>	<b>93.33</b>	<b>90.00</b>	<b>95.50</b>	<b>91.62</b>

TABLE II

PERFORMANCE COMPARISONS OF QUALITY EVALUATION METHODS FROM PERSPECTIVES OF PERCEPTUAL QUALITY, EDITING ALIGNMENT, AND ATTRIBUTE PRESERVATION. SRCC ( $\rho_s$ ), KRCC ( $\rho_k$ ), AND PLCC ( $\rho_p$ ) ARE REPORTED. ♠ TRADITIONAL FR IQA METRICS, ♡ DEEPCODE BASELINES, ♢ DEEP LEARNING-BASED FR IQA METHODS, ♦ DEEP LEARNING-BASED NR IQA METHODS, ★ VISION-LANGUAGE METHODS, ☆ LMM-BASED MODELS. THE FINE-TUNED RESULTS ARE MARKED WITH \*. THE BEST RESULTS ARE HIGHLIGHTED IN **RED**, AND THE SECOND-BEST RESULTS ARE HIGHLIGHTED IN **BLUE**.

Dimensions Methods/Metrics	Quality	Alignment	Preservation
★MSE	0.0268	0.0191	0.2215
★PSNR	0.0245	0.0169	0.2228
★SSIM [38]	0.0038	0.0027	0.1655
★FSIM [39]	0.0508	0.0326	0.2347
★BIOI [40]	0.3182	0.1867	0.3335
★DIVINE [41]	0.1541	0.0918	0.3639
★BRISQUE [42]	0.3699	0.2432	0.3868
★LPIPS [10]	0.1903	0.1351	0.3024
★ST-LPIPS [43]	0.0054	0.0045	0.0482
★CVRKD* [44]	0.7740	0.6128	<b>0.8807</b>
★AHIQ* [45]	0.7528	0.6367	0.7575
◊DBCNN* [46]	0.7294	0.6800	0.7997
◊HyperIQ* [47]	0.7110	0.4972	0.6919
◊MANIQ* [48]	0.7955	<b>0.6814</b>	0.8544
◊TOPIC* [49]	0.8026	0.6180	0.7919
◊Q-Algn* [9]	<b>0.8527</b>	0.8528	0.8793
★CLIPScore [50]	0.2024	0.1326	0.2417
★ImageReward [51]	0.4288	0.2588	0.3979
★PicScore [52]	0.2586	0.1562	0.2683
★LlaVascore [53]	0.3154	0.1934	0.3668
★QVascore [54]	0.2796	0.2150	0.3250
★LLaVA-1.5 (7B) [29]	0.1402	0.1149	0.2317
★LLaVA-NeXT (8B) [30]	0.0818	0.0675	0.0131
★mPLUG-Owl3 (7B) [31]	0.2002	0.1384	0.0347
★LLama3.2-Vision (11B) [32]	0.0818	0.0675	0.1213
★MiniCPM-V2.6 (8B) [33]	0.2706	0.2198	0.3094
★InternVL3 (8B) [55]	0.4629	0.3655	0.2437
★DeepSeekVL2 (small) [56]	0.2577	0.2104	0.2207
★Qwen3-VL (7B) [37]	0.5822	0.4427	0.5090
★LLaVA-NeXT (8B)* [30]	0.8161	0.6634	0.8249
★DeepSeekVL2 (small)* [56]	0.8054	0.6430	0.8273
★Qwen3-VL (8B)* [37]	0.8377	0.6520	0.8331
Ours	<b>0.8687</b>	<b>0.7430</b>	<b>0.8852</b>

TABLE III

COMPARISONS OF THE ALIGNMENT BETWEEN DIFFERENT EVALUATION METHODS AND HUMAN PERCEPTION IN EDITING MODELS. THE BEST RESULTS ARE HIGHLIGHTED IN **RED**, AND THE SECOND-BEST RESULTS ARE HIGHLIGHTED IN **BLUE**. **\*** DENOTES FINE-TUNED MODELS.

Dimensions/ Models/Metrics	Perceptual Quality					Editing Alignment					Attribute Preservation					Overall Rank	
	Human	Ours <sup>*</sup>	Qwen3-VL	Q-Align <sup>*</sup>	MANIQA <sup>*</sup>	Human	Ours <sup>*</sup>	Qwen3-VL	Q-Align <sup>*</sup>	PickScore	Human	Ours <sup>*</sup>	Qwen3-VL	AHQIQ <sup>*</sup>	LPIPS	Human	Ours
FlowEdit(SD3) [23]	62.09	61.25	90.12	56.79	0.754	59.65	51.42	91.78	0.584	0.905	57.57	51.67	90.12	0.631	1.924	1	1
RFSE [22]	61.80	61.58	88.52	58.63	0.790	55.77	52.13	88.41	0.527	0.903	50.71	46.67	85.00	0.569	3.676	2	2
ACE++ [1]	59.15	59.29	88.41	56.08	0.773	52.87	55.63	91.78	0.597	0.872	48.26	41.67	85.04	0.357	9.697	3	3
CDS [18]	64.15	63.83	95.19	60.88	0.680	34.50	37.04	95.12	0.529	0.904	67.23	60.00	95.15	0.805	0.215	4	6
FlowEdit(FLUX) [23]	56.43	58.75	90.12	52.88	0.740	42.22	49.38	90.08	0.583	0.905	51.18	48.33	88.37	0.611	2.397	5	4
InfEdit [20]	51.47	53.38	91.82	47.88	0.667	40.15	41.96	93.45	0.512	0.896	56.22	53.33	91.82	0.747	1.214	6	7
PnP [19]	56.71	55.54	90.12	52.38	0.661	36.00	40.63	95.19	0.539	0.904	57.41	50.00	85.00	0.670	1.941	7	11
Any2Pix [11]	54.31	62.00	88.63	57.46	0.771	44.93	53.00	90.23	0.689	0.833	44.36	41.67	86.71	0.432	8.131	8	5
Magicbrush [3]	52.50	56.71	93.53	60.50	0.67	37.69	39.00	93.49	0.503	0.898	57.13	55.00	88.45	0.728	1.781	9	8
EDICT [15]	49.67	53.54	90.08	47.71	0.622	39.09	41.13	90.04	0.468	0.857	55.61	53.33	90.12	0.756	0.643	10	9
ZONE [12]	53.40	58.83	94.04	50.83	0.689	34.79	36.42	94.00	0.502	0.906	59.23	56.67	94.07	0.808	0.592	11	10
IP2P [2]	49.43	55.96	91.78	48.77	0.659	40.57	41.71	91.71	0.460	0.846	51.18	45.00	81.74	0.661	3.122	12	12
ReNoise [21]	44.80	47.65	72.54	41.47	0.604	41.90	43.46	72.50	0.425	0.826	48.44	43.33	70.83	0.567	3.721	13	14
HQEdit [13]	45.84	52.13	86.93	43.29	0.653	43.87	49.96	88.41	0.500	0.793	39.77	36.67	63.37	0.413	7.486	14	13
DDPM [16]	43.90	47.00	83.37	35.77	0.544	37.96	39.92	83.37	0.433	0.631	48.37	46.67	75.04	0.654	2.637	15	15
MasaCtrl [17]	41.56	42.58	83.37	33.13	0.448	39.85	41.92	78.41	0.486	0.890	47.14	46.67	76.71	0.547	3.152	16	16
Text2LIVE [14]	32.68	34.02	83.37	28.90	0.323	34.16	37.54	86.71	0.350	0.896	44.64	43.33	83.37	0.592	1.733	17	17
SRCC to human $\uparrow$	<b>0.909</b>	0.579	<b>0.892</b>	0.875		<b>0.953</b>	0.239	<b>0.465</b>	0.175		<b>0.904</b>	0.746	<b>0.847</b>	0.748	<b>0.956</b>		
RMSE to human $\downarrow$	<b>3.720</b>	37.15	<b>4.578</b>	51.71		<b>4.236</b>	47.91	42.22	<b>41.88</b>		<b>4.341</b>	<b>32.57</b>	51.80	49.60	<b>1.455</b>		

TABLE IV

ABLATION STUDY ON THE DIFFERENT BACKBONES, DECODERS AND LORA TUNING STRATEGY.

Backbone & Strategy	Detection		Quality		Alignment		Preservation		Backbone	Decoders	LoRA(vision)	LoRA(lm)	LSA	Acc $\uparrow$	F1 $\uparrow$	$\rho_s \uparrow$	$\rho_p \uparrow$	$\rho_p \uparrow$
	Human	Ours <sup>*</sup>	Human	Ours <sup>*</sup>	Human	Ours <sup>*</sup>	Human	Ours <sup>*</sup>										
InternVL3.5 [36]	✓	✓	86.4	88.1	0.754	0.788	0.738	0.760	0.745	0.771								
InternVL3.5 [36]	✓	✓	86.4	87.5	0.780	0.803	0.764	0.780	0.746	0.789								
InternVL3.5 [36]	✓	✓	89.4	90.0	0.810	0.822	0.809	0.810	0.786	0.785								
InternVL3.5 [36]	✓	✓	91.5	91.6	0.838	0.850	0.827	0.856	0.822	0.835								
InternVL3.5 [36]	✓	✓	90.4	91.6	0.827	0.885	0.859	0.861	0.887	0.895								
InternVL3 [55]	✓	✓	87.2	89.4	0.805	0.827	0.836	0.832	0.839	0.832								
DeepSedL2 [35]	✓	✓	91.8	90.0	0.837	0.833	0.847	0.848	0.833	0.833								
Qwen3-VL [37]	✓	✓	91.8	90.0	0.837	0.833	0.847	0.848	0.833	0.833								

multiple dimensions, fully agreeing with human consensus. This demonstrates the reliability of our metric for real-world model comparison and benchmarking.

#### D. Ablation Studies

To verify the effectiveness of each component in our framework, we conducted a comprehensive ablation study using the InternVL3.5 backbone. The results are detailed in Table IV.

1) *Impact of Visual Tuning:* We compare the baseline setting using only LLM LoRA and decoders against the dual LoRA setting. The introduction of contrastive visual tuning yields substantial improvement in detection accuracy and increases the quality correlation ( $\rho_s$ ). This result confirms that standard MLLM are inherently insensitive to high-frequency editing artifacts, and our visual tuning strategy successfully injects this necessary forensic capability.

2) *Effectiveness of Layer Sensitivity Analysis:* The proposed Layer Sensitivity Analysis (LSA) provides the final and most significant performance enhancement. By comparing without LSA and the full model with LSA, we observe that the detection accuracy increases from 91.5% to 95.5%, accompanied by consistent improvements across all quality dimensions. This result verifies that the automatically selected intermediate layer offers a superior balance between low-level forensic cues and high-level semantic information.

3) *Generalization Across Backbones:* To verify the universality of our framework, we applied our strategy to different backbones. Our method consistently achieves high performance on Qwen3-VL and InternVL3 backbone, demonstrating that our visual tuning and LSA mechanisms are model-agnostic and can be generalized to various MLLM backbones.

## V. CONCLUSION

In this paper, we introduce HPE-Bench, a fine-grained benchmark designed for forensic supervision and instruction-aware analysis of human pose editing. Building upon this benchmark, we present a unified evaluation framework that jointly addresses authenticity detection and multi-dimensional quality assessment for fine-grained human pose editing results. Extensive experiments demonstrate that the proposed framework achieves state-of-the-art performance.

## REFERENCES

- Chaojie Mao, Jingfeng Zhang, Yulin Pan, Zeyinzi Jiang, Zhen Han, Yu Liu, et al., “Ace++: Instruction-based image creation and editing via context-aware content filling,” *arXiv preprint:2501.02487*, 2025.
- Tim Brooks, Aleksander Holynski, and Alexei A Efros, “Instructpix2pix: Learning to follow image editing instructions,” in *Proceedings of the IEEE/CVF Conference on Computer Vision and Pattern Recognition (CVPR)*, 2023, pp. 18392–18402.
- Kai Zhang, Lingbo Mo, Wenhui Chen, Huan Sun, and Yu Su, “Magicbrush: A manually annotated dataset for instruction-guided image editing,” in *Proceedings of the Advances in Neural Information Processing Systems (NeurIPS)*, 2023.
- Yanzuo Lu, Manlin Zhang, Andy J Ma, Xiaohua Xie, and Jianhuang Lai, “Coarse-to-fine latent diffusion for pose-guided person image synthesis,” in *Proceedings of the IEEE/CVF Conference on Computer Vision and Pattern Recognition*, 2024, pp. 6420–6429.
- Chengbo Dong, Xinru Chen, Ruohan Hu, Juan Cao, and Xirong Li, “Mvss-net: Multi-view multi-scale supervised networks for image manipulation detection,” *IEEE Transactions on Pattern Analysis and Machine Intelligence (TPAMI)*, vol. 45, no. 3, pp. 3539–3553, 2022.
- Xiaohong Liu, Yaojie Liu, Jun Chen, and Xiaoming Liu, “Psc-net: Progressive spatio-channel correlation network for image manipulation detection and localization,” *IEEE Transactions on Circuits and Systems for Video Technology (TCSVT)*, vol. 32, no. 11, pp. 7505–7517, 2022.
- Zitong Xu, Haoran Duan, Bowen Liu, Guoqiang Ma, Jiahao Wang, Lin Yang, and Wei Lin, “Lmm4edit: Benchmarking and evaluating multimodal image editing with lmms,” in *Proceedings of the ACM International Conference on Multimedia (ACM MM)*, October 2025.
- Zhipeng Xu, Xuanyu Zhang, Runyi Li, Zecheng Tang, Qing Huang, and Jian Zhang, “Fakeshield: Explainable image forgery detection and localization via multi-modal large language models,” in *Proceedings of the International Conference on Learning Representations (ICLR)*, 2025.
- Haoning Wu, Zicheng Zhang, Weixia Zhang, Chaofeng Chen, Chunyi Li, Liang Liao, et al., “Q-align: Teaching lmms for visual scoring via discrete text-defined levels,” *arXiv preprint:2312.17090*, 2023.
- R. Zhang, P. Isola, A. A. Efros, E. Shechtman, and O. Wang, “The unreasonable effectiveness of deep features as a perceptual metric,” in *Proceedings of the IEEE/CVF Conference on Computer Vision and Pattern Recognition (CVPR)*, 2018.
- Shufan Li, Harkarwar Singh, and Aditya Grover, “Instructany2pix: Flexible visual editing via multimodal instruction following,” *arXiv preprint:2312.06738*, 2023.

[12] Shanglin Li, Bohan Zeng, Yutang Feng, Sicheng Gao, Xuhui Liu, Jiaming Liu, et al., “Zone: Zero-shot instruction-guided local editing,” *arXiv preprint:2312.16794*, 2023.

[13] Mude Hui, Siwei Yang, Bingchen Zhao, Yichun Shi, Heng Wang, Peng Wang, et al., “Hq-edit: A high-quality dataset for instruction-based image editing,” *arXiv preprint:2404.09990*, 2024.

[14] Omer Bar-Tal, Dolev Ofri-Amar, Rafail Fridman, Yoni Kasten, and Tali Dekel, “Text2live: Text-driven layered image and video editing,” in *Proceedings of the European Conference on Computer Vision (ECCV)*, 2022, pp. 707–723.

[15] Bram Wallace, Akash Gokul, and Nikhil Naik, “Edict: Exact diffusion inversion via coupled transformations,” *arXiv preprint:2211.12446*, 2022.

[16] Inbar Huberman-Spiegelglas, Vladimir Kulikov, and Tomer Michaeli, “An edit friendly DDPM noise space: Inversion and manipulations,” in *Proceedings of the IEEE/CVF Conference on Computer Vision and Pattern Recognition (CVPR)*, 2024, pp. 12469–12478.

[17] Mingdeng Cao, Xintao Wang, Zhongang Qi, Ying Shan, Xiaohu Qie, and Yingqiang Zheng, “Masactrl: Tuning-free mutual self-attention control for consistent image synthesis and editing,” in *Proceedings of the IEEE/CVF international conference on computer vision (CVPR)*, 2023.

[18] Hyelin Nam, Gihyun Kwon, Geon Yeong Park, and Jong Chul Ye, “Contrastive denoising score for text-guided latent diffusion image editing,” in *Proceedings of the IEEE/CVF Conference on Computer Vision and Pattern Recognition (CVPR)*, June 2024, pp. 9192–9201.

[19] Xuan Ju, Ailing Zeng, Yuxuan Bian, Shaoteng Liu, and Qiang Xu, “Pnp inversion: Boosting diffusion-based editing with 3 lines of code,” in *Proceedings of the International Conference on Learning Representations (ICLR)*, 2024.

[20] Sihan Xu, Yidong Huang, Jiayi Pan, Ziqiao Ma, and Joyce Chai, “Inversion-free image editing with natural language,” in *Proceedings of the IEEE/CVF Conference on Computer Vision and Pattern Recognition (CVPR)*, 2024, pp. 9192–9201.

[21] Daniel Garibi, Or Patashnik, Andrey Voynov, Hadar Averbuch-Elor, and Daniel Cohen-Or, “Renoise: Real image inversion through iterative noising,” *arXiv preprint:2403.14602*, 2024.

[22] Jiangshan Wang, Junfu Pu, Zhongang Qi, Jiayi Guo, Yue Ma, Nisha Huang, Yuxin Chen, Xiu Li, and Ying Shan, “Taming rectified flow for inversion and editing,” *arXiv preprint:2411.04746*, 2024.

[23] Vladimir Kulikov, Matan Kleiner, Inbar Huberman-Spiegelglas, and Tomer Michaeli, “Flowedit: Inversion-free text-based editing using pre-trained flow models,” *arXiv preprint:2412.08629*, 2024.

[24] Xiao Guo, Xiaohong Liu, Zhiyuan Ren, Steven Grosz, Iacopo Masi, and Xiaoming Liu, “Hierarchical fine-grained image forgery detection and localization,” in *Proceedings of the IEEE/CVF Conference on Computer Vision and Pattern Recognition (CVPR)*, 2023.

[25] Sheng-Yu Wang, Oliver Wang, Richard Zhang, Andrew Owens, and Alexei A Efros, “Cnn-generated images are surprisingly easy to spot... for now,” in *Proceedings of the IEEE/CVF Conference on Computer Vision and Pattern Recognition (CVPR)*, 2020, pp. 8695–8704.

[26] Chuangchuang Tan, Yao Zhao, Shikui Wei, Guanghua Gu, and Yunchao Wei, “Learning on gradients: Generalized artifacts representation for gan-generated images detection,” in *Proceedings of the IEEE/CVF Conference on Computer Vision and Pattern Recognition (CVPR)*, 2023.

[27] Utkarsh Ojha, Yuheng Li, and Yong Jae Lee, “Towards universal fake image detectors that generalize across generative models,” in *Proceedings of the IEEE/CVF Conference on Computer Vision and Pattern Recognition (CVPR)*, 2023, pp. 24480–24489.

[28] Shilin Yan, Ouxiang Li, Jiayin Cai, Yanbin Hao, Xiaolong Jiang, Yao Hu, et al., “A sanity check for ai-generated image detection,” *arXiv preprint:2406.19435*, 2024.

[29] Haotian Liu, Chunyuan Li, Yuheng Li, and Yong Jae Lee, “Improved baselines with visual instruction tuning,” in *Proceedings of the IEEE/CVF Conference on Computer Vision and Pattern Recognition (CVPR)*, 2024, pp. 26296–26306.

[30] Feng Li, Renrui Zhang, Hao Zhang, Yuanhan Zhang, Bo Li, Wei Li, et al., “Llava-next-interleave: Tackling multi-image, video, and 3d in large multimodal models,” *arXiv preprint:2407.07895*, 2024.

[31] Jiabo Ye, Haiyang Xu, Huawei Liu, Anwen Hu, Ming Yan, Qi Qian, et al., “mplug-owl3: Towards long image-sequence understanding in multimodal large language models,” in *Proceedings of the International Conference on Learning Representations (ICLR)*, 2024.

[32] AI Meta, “Llama 3.2: Revolutionizing edge ai and vision with open, customizable models,” *Meta AI Blog*, December 2024.

[33] Yuan Yao, Tianyu Yu, Ao Zhang, Chongyi Wang, Junbo Cui, Hongji Zhu, et al., “Minicpm-v: A gpt-4v level mlm on your phone,” *arXiv preprint:2408.01800*, 2024.

[34] Shiyin Lu, Yang Li, Yu Xia, Yuwei Hu, Shanshan Zhao, Yanqing Ma, et al., “Ovis2.5 technical report,” *arXiv:2508.11737*, 2025.

[35] DeepSeek-AI, Aixin Liu, Bei Feng, Bin Wang, Bingxuan Wang, Bo Liu, Chenggang Zhao, et al., “Deepseek-v2: A strong, economical, and efficient mixture-of-experts language model,” *arXiv preprint:2405.04434*, 2024.

[36] Weiyun Wang, Zhangwei Gao, Lixin Gu, Hengjun Pu, Long Cui, Xingguang Wei, Zhaoyang Liu, Linglin Jing, Shenglong Ye, Jie Shao, et al., “Internvl3.5: Advancing open-source multimodal models in versatility, reasoning, and efficiency,” *arXiv preprint:2508.18265*, 2025.

[37] An Yang, Anfeng Li, Baosong Yang, Beichen Zhang, Binyuan Hui, Bo Zheng, et al., “Qwen3 technical report,” *arXiv preprint:2505.09388*, 2025.

[38] Z. Wang, A. C. Bovik, H. R. Sheikh, and E. P. Simoncelli, “Image quality assessment: from error visibility to structural similarity,” *IEEE Transactions on Image Processing (TIP)*, vol. 13, no. 4, 2004.

[39] L. Zhang, L. Zhang, X. Mou, and D. Zhang, “Fsim: A feature similarity index for image quality assessment,” *IEEE Transactions on Image Processing (TIP)*, vol. 20, no. 8, pp. 2378–2386, 2011.

[40] A. K. Moorthy and A. C. Bovik, “A modular framework for constructing blind universal quality indices,” *IEEE Signal Processing Letters (SPL)*, 2009.

[41] Anush Krishna Moorthy and Alan Conrad Bovik, “Blind image quality assessment: From natural scene statistics to perceptual quality,” *IEEE Transactions on Image Processing (TIP)*, vol. 20, no. 12, 2011.

[42] Anish Mittal, Anush K. Moorthy, and Alan C. Bovik, “Blind/referenceless image spatial quality evaluator,” in *Proceedings of the Asilomar Conference on Signals, Systems and Computers (ACSSC)*, 2011, pp. 723–727.

[43] Abhijay Ghildyal and Feng Liu, “Shift-tolerant perceptual similarity metric,” in *Proceedings of the European Conference on Computer Vision (ECCV)*, 2022, p. 91–107.

[44] Guanghao Yin, Wei Wang, Zehuan Yuan, Chuchu Han, Wei Ji, Shouqian Sun, et al., “Content-variant reference image quality assessment via knowledge distillation,” in *Proceedings of the Conference on Association for the Advancement of Artificial Intelligence (AAAI)*, 2022, vol. 36.

[45] Shanshan Lao, Yuan Gong, Shuwei Shi, Sidi Yang, Tianhe Wu, Jiahao Wang, et al., “Attentions help cnns see better: Attention-based hybrid image quality assessment network,” in *Proceedings of the IEEE/CVF Conference on Computer Vision and Pattern Recognition (CVPR) Workshops*, 2022, pp. 1140–1149.

[46] W. Zhang, K. Ma, J. Yan, D. Deng, and Z. Wang, “Blind image quality assessment using a deep bilinear convolutional neural network,” *IEEE Transactions on Circuits and Systems for Video Technology (TCSVT)*, vol. 30, no. 1, pp. 36–47, 2020.

[47] S. Su, Q. Yan, Y. Zhu, C. Zhang, X. Ge, J. Sun, et al., “Blindly assess image quality in the wild guided by a self-adaptive hyper network,” in *Proceedings of the IEEE/CVF Conference on Computer Vision and Pattern Recognition (CVPR)*, June 2020.

[48] Sidi Yang, Tianhe Wu, Shuwei Shi, Shanshan Lao, Yuan Gong, Mingdeng Cao, et al., “Maniq: Multi-dimension attention network for no-reference image quality assessment,” in *Proceedings of the IEEE/CVF Conference on Computer Vision and Pattern Recognition (CVPR)*, 2022.

[49] Chaofeng Chen, Jiadi Mo, Jingwen Hou, Haoning Wu, Liang Liao, Wenxiu Sun, Qiong Yan, and Weisi Lin, “Topiq: A top-down approach from semantics to distortions for image quality assessment,” *IEEE Transactions on Image Processing (TIP)*, vol. 33, pp. 2404–2418, 2024.

[50] Jack Hessel, Ari Holtzman, Maxwell Forbes, Ronan Le Bras, and Yejin Choi, “Clipscore: A reference-free evaluation metric for image captioning,” *arXiv preprint:2104.08718*, 2021.

[51] Jiazheng Xu, Xiao Liu, Yuchen Wu, Yuxuan Tong, Qinkai Li, Ming Ding, et al., “Imagereward: learning and evaluating human preferences for text-to-image generation,” in *Proceedings of the International Conference on Neural Information Processing Systems (NeurIPS)*, 2023.

[52] Yuval Kirstain, Adam Polyak, Uriel Singer, Shahbuland Matiana, Joe Penna, and Omer Levy, “Pick-a-pic: An open dataset of user preferences for text-to-image generation,” in *Proceedings of the Advances in Neural Information Processing Systems (NeurIPS)*, 2023, pp. 36652–36663.

[53] Yuheng Li, Haotian Liu, Mu Cai, Yijun Li, Eli Shechtman, Zhe Lin, et al., “Removing distributional discrepancies in captions improves image-text alignment,” *arXiv preprint:2410.00905*, 2024.

- [54] Baiqi Li, Zhiqiu Lin, Deepak Pathak, Jiayao Li, Yixin Fei, Kewen Wu, et al., “Evaluating and improving compositional text-to-visual generation,” in *Proceedings of the IEEE/CVF Conference on Computer Vision and Pattern Recognition (CVPR)*, 2024.
- [55] Jinguo Zhu, Weiyun Wang, Zhe Chen, Zhaoyang Liu, Shenglong Ye, Lixin Gu, et al., “Internvl3: Exploring advanced training and test-time recipes for open-source multimodal models,” *arXiv preprint:2504.10479*, 2025.
- [56] Zhiyu Wu, Xiaokang Chen, Zizheng Pan, Xingchao Liu, Wen Liu, Damai Dai, et al., “Deepseek-vl2: Mixture-of-experts vision-language models for advanced multimodal understanding,” *arXiv preprint:2412.10302*, 2024.
- [57] Zhaolin Cai, Fan Li, Ziwei Zheng, and Yanjun Qin, “Hiprobe-vad: Video anomaly detection via hidden states probing in tuning-free multimodal llms,” in *Proceedings of the ACM International Conference on Multimedia*, 2025, p. 592–601.
- [58] Zhaolin Cai, Fan Li, Ziwei Zheng, Haixia Bi, and Lijun He, “Headhunt-vad: Hunting robust anomaly-sensitive heads in mllm for tuning-free video anomaly detection,” *arXiv preprint:2512.17601*, 2025.